
Experimental Investigation of Mechanics in Soft-fingered Grasping and Manipulation

Takaniro Inoue and Shinichi Hirai

Dept. Robotics, Ritsumeikan Univ.,
Kusatsu, Shiga 525-8577, Japan
hirai@se.ritsumei.ac.jp
<http://www.ritsumei.ac.jp/se/~hirai/>

Summary. This paper describes mechanical modeling of soft-fingered grasping and manipulation. Here, we used a simple hand consisting of a pair of 1-DOF rotational fingers with hemispherical soft fingertips to investigate the mechanics of soft-fingered grasping and manipulation. Based on the observations of soft-fingered grasping and manipulation, we propose a parallel distributed model with tangential deformation of hemispherical soft fingertips. We experimentally verified our proposed parallel distributed model. We then show that simulation results based on the parallel distributed model agree with the observations well.

1 Introduction and State-of-the-Art

Human fingertips consist of soft tissue and this softness is one source of dexterity in grasping and manipulation of objects. The softness yields area-contact between each fingertip and an object, which allows stable grasping and manipulation. Therefore, robotics research has focused on the mechanics of soft-fingered grasping and manipulation.

In this paper, we focus on a mechanical model of hemispherical soft fingertips based on observation of soft-fingered grasping and manipulation. To examine the mechanics of grasping and manipulation by soft fingertips, we used a simple hand consisting of a pair of 1-DOF rotational fingers with hemispherical soft fingertips. The deformation properties of soft fingertips may be observed clearly in such a simple hand system, which will aid in determining the mechanics of soft-fingered grasping and manipulation.

Finite element (FE) analysis is often applied to study deformation of objects. Xydas and Kao reported the exact deformation shape of a hemispherical soft fingertip using FE analysis [1, 2, 3]. FE analysis can be used to simulate the process of grasping and manipulation numerically but cannot be applied to theoretical analysis of grasping and manipulation due to its complex formulation. For example, graspability of an object and stability in the dynamic manipulation process are key theoretical concepts in grasping and manipulation.

FE analysis yields a *procedural* model of deformation. Use of the numerical procedure allows simulation of the deformation of objects but unfortunately, such procedural models cannot be applied to theoretical analysis. According to the principle of Occam’s razor, we should choose a simple model to analyze and explain grasping and manipulation by soft fingertips.

The Hertzian contact model provides a simple closed-form description of the contact between two quadratic surfaces of elastic objects [4]. The model assumes that surfaces are open-ended, and thus the model cannot be applied to a hemispherical elastic fingertip subtended by a rigid plate. Arimoto *et al.* formulated dynamics in pinching by a pair of soft fingertips [5]. They applied a radially distributed deformation model of a soft fingertip to allow use of analytical mechanics theory in control [6]. Based on the concept of *stability on a manifold*, they showed theoretically that a pair consisting of a 2-DOF finger and a 1-DOF finger can realize secure grasping and posture control [7, 8]. They also showed that *rolling contact* between an object and fingertips is the key to stable grasping and posture control. Then, the third DOF is needed to achieve the equilibrium of moments acting on a grasped object. However, our observations described in the following section suggest that a pair of 1-DOF fingers with soft fingertips can perform both secure grasping and posture control. Thus, a new model of soft fingertips is needed to resolve this discrepancy.

2 Observation of Soft-fingered Grasping and Manipulation

2.1 Object pinching by a pair of 1-DOF fingers

Let us observe the grasping and manipulation of a rigid object by a pair of fingers with soft fingertips. Each finger has one rotational joint driven by an actuator. First, let us move the two fingertips inward, that is, toward each other, and observe their deformation. Figure 1 shows a photograph of the object and the fingertips. As the two joints rotate inward, both fingertips show a greater degree of deformation, implying an increase in grasping force applied to the object. This observation suggests that the grasping force can be regulated by the two joint angles, *i.e.*, secure grasping can be achieved by a pair of 1-DOF fingers with soft fingertips. Next, let us move one fingertip inward and the other outward to observe the orientation of an object. That is, two fingers rotate in the same direction. Figure 2 shows a photograph of the object and the fingertips. As shown in the figure, the object rotates clockwise when the two fingers rotate counterclockwise and *vice versa*, implying that the object orientation can be regulated by the two joint angles. This observation suggests that orientation control can be achieved by a pair of 1-DOF fingers with soft fingertips. We should emphasize that the object rotates in the opposite direction to the rotation of the two fingers.

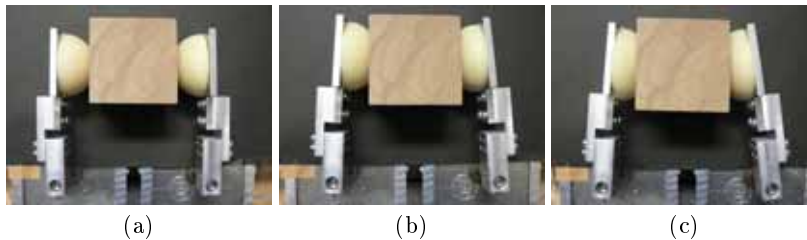


Fig. 1. Deformation of fingertips when two fingers rotate in the opposite direction

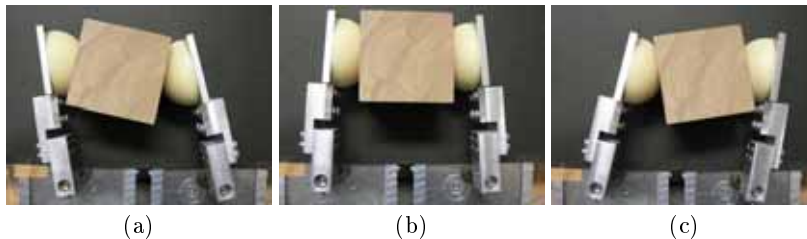


Fig. 2. Motion of object when two fingers rotate in the same direction

The above observations suggest that a pair of 1-DOF fingers with soft fingertips can control both grasping force and object orientation independently. Arimoto *et al.* analyzed the dynamics of soft-fingered grasping and manipulation and concluded that a pair of 1-DOF rotational fingers with soft fingertips can control grasping force but not object orientation. They asserted that a combination of a 1-DOF finger and a 2-DOF finger is required to control both grasping force and object orientation. Thus, there is a discrepancy between our observations and their analysis. They applied a radially distributed model of soft fingertips to the analysis, which is described in Figure 4-(a). The contact force passes the center of a hemisphere. The magnitude of the force is dependent on the maximum displacement of the soft fingertip but not on the relative orientation between the object and the fingertip. Contact forces caused by two radially distributed models apply a non-zero moment to the object, implying that an additional DOF is needed to cancel out the moment and to stabilize the object rotation. Therefore, another fingertip model is needed, which is dependent on both the maximum displacement and the relative orientation between the object and the fingertip.

2.2 Rotation of pinched object by external force

Let us pinch an object by two fingers fixed at given orientations and observe the motion of the object caused by an external force applied to the object. Figure 3 shows a photograph of the object. As the fingertips deform, the grasped object may rotate due to the applied force. With release of the applied force, the object rotates back to the initial orientation, implying that

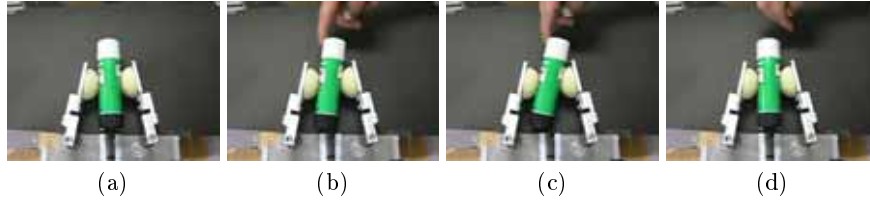


Fig. 3. Pinched object rotation by external force

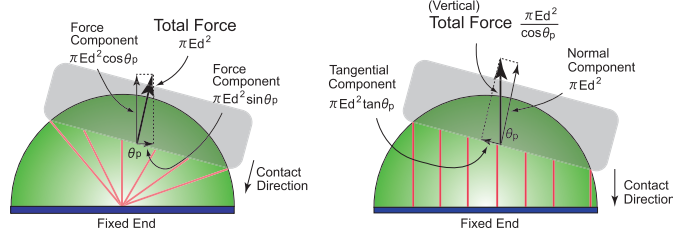
the object does not slip on the fingertip surfaces. This yields geometric constraints, which are referred to as *rolling constraints*. Giving constant values to both joint angles and solving the two rolling constraints, we find that the orientation of the grasped object is constant. Here, we found another discrepancy between our observations and the analysis reported by Arimoto *et al.* In the radially distributed model, any point on the hemispherical surface of a soft fingertip moves along a line, which determines the shrinkage of an elastic element inside the fingertip. That is, each elastic element deforms normally but not tangentially. The above discrepancy is due to this lack of tangential deformation of the fingertip. To describe the rotation of a pinched object by an external force, it is necessary to introduce tangential deformation into the fingertip model.

3 Soft Fingertip Models

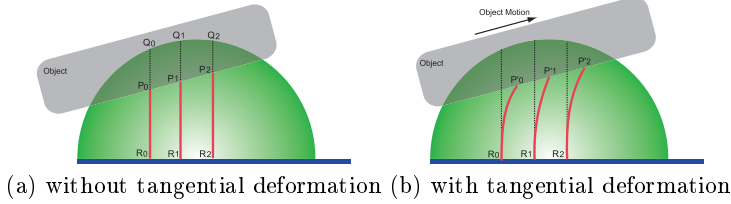
We build a model of soft fingertips based on the observations described in Section 2. Figure 4-(a) shows the radially distributed model, which has been applied previously to the analysis of soft-fingered grasping and manipulation. Let a be the radius of a hemispherical fingertip in its natural shape and E be Young's modulus of the material of the fingertip. Elastic elements are distributed radially inside the fingertip. As all elements have the same natural length, which is given by the radius a of the fingertip, all elements have the same spring constant $E dS/a$, where dS denotes the cross-sectional area of the element. Contact between the soft fingertip and the planar surface of a rigid object results in deformation of the fingertip, and thus an elastic force being applied to the object by the finger. Let d be the maximum displacement of the soft fingertip and θ_p be the relative orientation between the fingertip and the object. Each elastic element generates an elastic force according to its shrinkage. Integrating all elastic forces provides the resultant contact force. Computing the integral, the magnitude of the contact force is given by

$$F_{\text{radial}} = \pi E d^2 \quad (1)$$

and the force passes the center of the fingertip, as illustrated in the figure. Note that the force magnitude depends on the maximum displacement d but is independent of the relative orientation θ_p .



(a) radially distributed model (b) parallel distributed model

Fig. 4. Fingertip models


(a) without tangential deformation (b) with tangential deformation

Fig. 5. Tangential deformation in the parallel distributed model

Figure 4-(b) shows our proposed parallel distributed model. Elastic elements are distributed in parallel inside a soft fingertip. Note that the natural length of each elastic element is dependent on the position of the element. Let (x, y) be the position of an elastic element. Then, its natural length is given by $(a^2 - x^2 - y^2)^{1/2}$, yielding the spring constant of the element given by $E dS / (a^2 - x^2 - y^2)^{1/2}$. Each elastic element generates an elastic force according to its shrinkage. Integrating all elastic forces provides the resultant contact force. Displacement d and angle θ_p determine the shrinkage of each elastic element. Computing the integral yields the magnitude of the contact force given by

$$F_{\text{perp}} = \frac{\pi E d^2}{\cos \theta_p} \quad (2)$$

and the force is perpendicular to the planar surface behind the fingertip, as illustrated in the figure. Note that the force magnitude depends on both the maximum displacement d and the relative orientation θ_p . This dependency is due to the hemispherical shape of the soft fingertip subtended by a fixed rigid end, which is similar to a human finger consisting of a soft fingertip and a hard fingernail. The parallel distributed model reflects this structure consisting of a soft fingertip and a hard fingernail.

Integrating potential energies caused by the perpendicular deformation of individual elastic elements in a parallel distributed model yields the potential energy of the fingertip as follows:

$$U_{\text{perp}}(d, \theta_p) = \frac{\pi E d^3}{3 \cos^2 \theta_p}. \quad (3)$$

Note that the potential energy depends not only on the maximum displacement d but also on the relative orientation θ_p .

As described in Section 2, tangential deformation should be introduced into the parallel distributed model so that a pinched object can rotate under the application of external force. Figure 5 shows the model of tangential deformation. Assume that the fingertip makes contact with the rigid object without tangential deformation of the fingertip, as illustrated in Figure 5-(a). In the parallel distributed model, point Q_k on the fingertip surface moves to P_k , shrinking the elastic element of natural length $Q_k R_k$ to $P_k R_k$. Assuming that the rigid object moves tangentially by displacement d_t as shown in Figure 5-(b), the point P_k moves to P'_k . Then, the elastic element has tangential deformation determined by $P_k P'_k$. Given the position and the orientation of an object, we can calculate the perpendicular deformation $Q_k P_k$ and tangential deformation $P_k P'_k$ of each elastic element. The tangential deformation determines the tangential force generated by the element. For the sake of simplicity, we assume that Young's modulus E characterizes the linear relationship between the tangential force and the tangential deformation. Integrating tangential forces at all elastic elements, we can derive the resultant tangential force as follows:

$$F_{\text{tangential}} = 2\pi E d d_t. \quad (4)$$

We should emphasize that perpendicular and lateral components of contact force in the radially distributed model are given by $F_{\text{radial}} \cos \theta_p$ and $F_{\text{radial}} \sin \theta_p$, respectively, which are different from the components in the parallel distributed model given by $F_{\text{perp}} + F_{\text{tangential}} \sin \theta_p$ and $F_{\text{tangential}} \cos \theta_p$. Integrating potential energies caused by tangential deformation of individual elastic elements in the parallel distributed model yields the total potential energy caused by tangential deformation as follows:

$$U_{\text{tangential}}(d, d_t, \theta_p) = \pi E \{d^2 d_t \tan \theta_p + d d_t^2\}. \quad (5)$$

As perpendicular and tangential displacements are not orthogonal, the above equation shows the coupling between them. Consequently, the total potential energy of a hemispherical soft fingertip in the parallel distributed model is formulated as follows:

$$U_{\text{parallel}}(d, d_t, \theta_p) = U_{\text{perp}}(d, \theta_p) + U_{\text{tangential}}(d, d_t, \theta_p). \quad (6)$$

Note that this potential energy is dependent on the maximum displacement d , the tangential displacement d_t , and the relative angle θ_p .

4 Experimental Verification

Let us experimentally verify the parallel distributed model proposed in Section 3. We have fabricated a hemispherical soft fingertip with a diameter of 40 mm

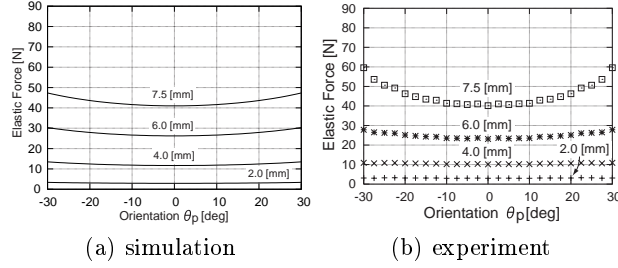


Fig. 6. Simulation and experimental results

and made of silicon rubber. We have conducted a tension and compression test to identify Young’s modulus of the silicon rubber as $E = 0.23$ MPa. An array of pressure sensors was applied to measure the force distribution behind the fingertip. The resultant perpendicular force can be computed by summing all pressure measurements. Figure 6 shows simulation and experimental results. The horizontal and vertical axes in the graphs denote the relative angle between the fingertip and an object and the magnitude of the elastic force, respectively. The maximum displacements are 2.0 mm, 4.0 mm, 6.0 mm, and 7.5 mm. As shown in Figure 6-(a), the magnitude of the contacting force reaches its minimum at $\theta_p = 0$ as long as the maximum displacement d remains constant. The experimental results shown in Figure 6-(b) also show that the magnitude reaches its minimum at $\theta_p = 0$. Consequently, the force model in the parallel distributed model agrees with the experimental results. Note that in the radially distributed model, the force magnitude remains constant and the component perpendicular to the plate behind the fingertip reaches its maximum rather than its minimum at $\theta_p = 0$. That is, the radially distributed model does not agree with the experimental results.

5 Simulation of Soft-fingered Grasping and Simulation

Based on the parallel distributed model, we simulated grasping and manipulation by a pair of 1-DOF fingers with soft fingertips. Figure 7 shows a simulation model. Let θ_l and θ_r be rotational angles of the left and right fingers. Assume that the two fingers have the same dimensions. Let L be the length between the center of the hemispherical fingertip and the joint of the finger. A pair of fingers pinches a rectangular object of width W_{obj} . Let (x_{obj}, y_{obj}) be the positional vector and θ_{obj} be the orientation angle of the pinched object. The relative angle between the object and the left finger is given by $\theta_r - \theta_{obj}$, while the angle between the object and the right finger is given by $\theta_l + \theta_{obj}$. Let d_l and d_{lt} be the maximum and tangential displacements of the left fingertip. The orientation of the left finger θ_l and the location of the object given by (x_{obj}, y_{obj}) and θ_{obj} determine these displacements. Let d_r and d_{rt} be the maximum and tangential displacements of the right fingertip, which

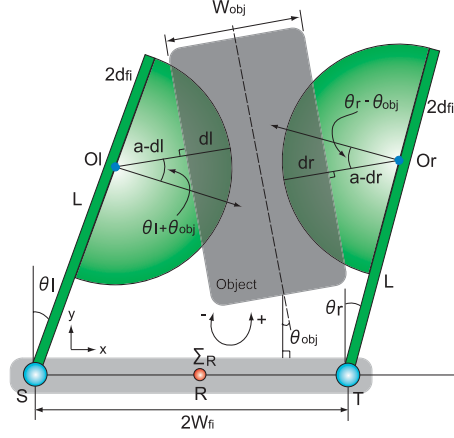


Fig. 7. Simulation model

are determined by the orientation of the right finger θ_r and the location of the object.

There are five generalized coordinates in the dynamics of grasping and manipulation by a pair of 1-DOF fingers: object position x_{obj} and y_{obj} , object orientation θ_{obj} , and the rotational angles of two fingers θ_l and θ_r . The maximum displacements d_l and d_r as well as tangential displacements d_{lt} and d_{rt} are described by functions of these five coordinates. Assume that fingers and an object move in the horizontal plane and that the gravitational energy is negligible. The potential energy of the system is given by the sum of elastic energies of the left and right fingertips as follows:

$$U = U_{\text{parallel}}(d_l, d_{lt}, \theta_l + \theta_{obj}) + U_{\text{parallel}}(d_r, d_{rt}, \theta_r - \theta_{obj}). \quad (7)$$

Let m_{obj} be the mass of the object and I_{obj} be the moment of inertia of the object around its center of gravity. Let I_{finger} be the moment of inertia of the finger around its rotational joint. Assuming that mass transfer due to the deformation of each fingertip is negligible, the kinetic energy of the system can then be formulated as

$$T = \frac{1}{2}m_{obj}(\dot{x}_{obj}^2 + \dot{y}_{obj}^2) + \frac{1}{2}I_{obj}\dot{\theta}_{obj}^2 + \frac{1}{2}I_{\text{finger}}\dot{\theta}_l^2 + \frac{1}{2}I_{\text{finger}}\dot{\theta}_r^2. \quad (8)$$

From eqs.(7) and (8), we can formulate the Lagrange equations of motion of a pair of fingers pinching a rigid object. We then introduce viscosity terms to equations.

Figure 8 shows a simulation of posture control of an object pinched by a pair of fingers. We used the identified Young's modules in the simulation. Figure 8-(a) shows the contact between the fingers and the object without fingertip deformation. Figure 8-(b) shows the initial grasping, where both fingertips have the same deformation. Both fingers rotate counterclockwise in

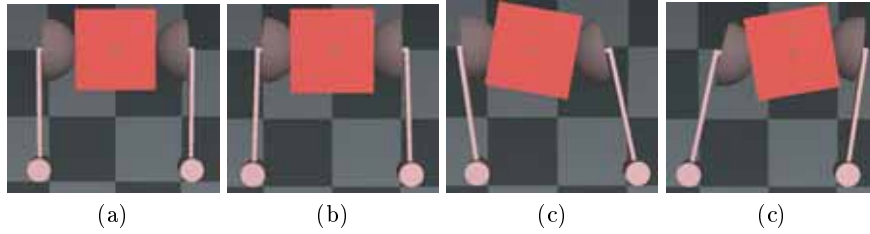


Fig. 8. Simulation of posture control of grasped object

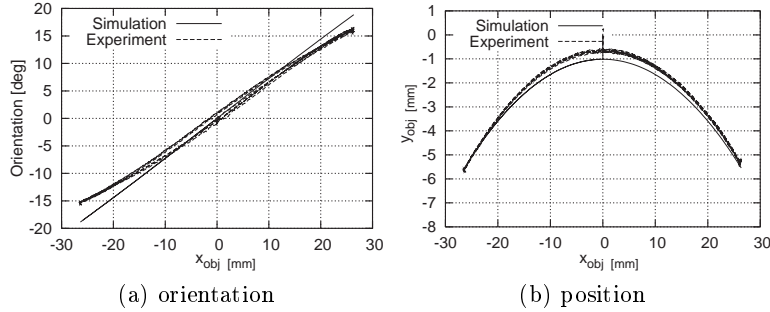


Fig. 9. Comparison between simulation and experimental results

Figure 8-(c), and the object rotates clockwise. Both fingers rotate clockwise in Figure 8-(d), and the object rotates counterclockwise. The simulation result based on the parallel distributed model agrees with the observation shown in Figure 2.

Figure 9 shows a comparison between simulation and experimental results in posture control of a pinched object. Figure 9-(a) shows the relationship between orientation angle θ_{obj} and coordinate x_{obj} of a pinched object. As shown in the figure, both results agree with each other, but the difference between the results increases as the orientation angle becomes larger. Figure 9-(b) shows the position of the pinched object. Simulation and experimental results agreed with each other.

From the above simulations, we conclude that our proposed parallel distributed model provides a good explanation of grasping and manipulation by soft fingertips.

6 Conclusion and Research Perspective

In this paper, we described modeling of hemispherical fingertips for soft-fingered grasping and manipulation. We used a simple hand consisting of a pair of 1-DOF rotational fingers with hemispherical soft fingertips to determine the mechanics of soft-fingered grasping and manipulation. First, we observed the

motion of a rigid object pinched by a pair of two 1-DOF fingers with hemispherical soft fingertips. Second, we formulated the radially distributed and parallel distributed models of soft fingertips. Third, we showed experimental results supporting the parallel distributed model proposed in this paper. Finally, we showed the simulations of soft-fingered grasping and manipulation based on the parallel distributed model. We found that the proposed model agrees with the observations.

We will conduct stability analysis of this grasping and manipulation in future studies and will apply the proposed model to the formulation of grasping and manipulation by a multi-DOF, multi-fingered hand to investigate the contribution of the fingernail to dexterity. The model proposed in this paper is planar. We will extend this planar model to a spatial model through observations of spatial grasping and manipulation.

Acknowledgement

This research was supported in part by the Ritsumeikan University 21st Century COE program “Micro Nanoscience Integrated Systems”.

References

1. Xydas, N. and Kao, I., *Modeling of Contact Mechanics and Friction Limit Surfaces for Soft Fingers in Robotics with Experimental Results*, Int. J. of Robotics Research, Vol. 18, No. 8, pp.941–950, 1999.
2. Xydas, N., Bhagavat, M., and Kao, I., *Study of Soft-Finger Contact Mechanics Using Finite Elements Analysis and Experiments*, Proc. IEEE Int. Conf. on Robotics and Automation, pp.2179–2184, 2000.
3. Kao, I. and Yang, F., *Stiffness and Contact Mechanics for Soft Fingers in Grasping and Manipulation*, IEEE Trans. on Robotics and Automation, Vol. 20, No. 1, pp.132–135, 2004.
4. Johnson, K. L., *Contact Mechanics*, Cambridge University Press, 1985.
5. Arimoto, S., Tahara, K., Yamaguchi, M, Nguyen, P, and Han, H. Y., *Principle of Superposition for Controlling Pinch Motions by means of Robot Fingers with Soft Tips*, Robotica, Vol. 19, pp.21–28, 2001.
6. Nguyen, P. and Arimoto, S, *Performance of Pinching Motions of Two Multi-DOF Robotic Fingers with Soft-Tips*, Proc. IEEE Int. Conf. on Robotics and Automation, pp.2344–2349, 2001.
7. Doulgeri, Z., Fasoulas, J., and Arimoto, S., *Feedback Control for Object Manipulation by a pair of Soft Tip Fingers*, Robotica, Vol. 20, pp.1–11, 2002.
8. Fasoulas, J. and Doulgeri, Z., *Equilibrium Conditions of a Rigid Object Grasped by Elastic Rolling Contacts*, Proc. IEEE Int. Conf. on Robotics and Automation, pp.789–794, 2004.